Casimir Effect for Curved Geometries: Proximity-Force-Approximation Validity Limits

Holger Gies and Klaus Klingmüller

Institut für Theoretische Physik, Philosophenweg 16, 69120 Heidelberg, Germany

(Received 20 January 2006; published 5 June 2006)

We compute Casimir interaction energies for the sphere-plate and cylinder-plate configuration induced by scalar-field fluctuations with Dirichlet boundary conditions. Based on a high-precision calculation using world-line numerics, we quantitatively determine the validity bounds of the proximity-force approximation (PFA) on which the comparison between all corresponding experiments and theory are based. We observe the quantitative failure of the PFA on the 1% level for a curvature parameter $a/R > 0.00755$. Even qualitatively, the PFA fails to predict reliably the correct sign of genuine Casimir curvature effects. We conclude that data analysis of future experiments aiming at a precision of 0.1% must no longer be based on the PFA.

DOI: 10.1103/PhysRevLett.96.220401 PACS numbers: 42.50.Lc, 03.70.+k, 11.10.−z

Measurements of the Casimir force [1] have reached a precision level of 1% [2–8]. Further improvements are currently aimed at with intense efforts, owing to the increasing relevance of these quantum forces for nano- and microscale mechanical systems; also, Casimir precision measurements play a major role in the search for new submillimeter forces, resulting in important constraints for new physics [9–13].

On this level of precision, corrections owing to material properties, thermal fluctuations, and geometry dependencies have to be accounted for [14–17]. In order to reduce material corrections such as surface roughness and finite conductivity which are difficult to control with high precision, force measurements at larger surface separations up to the micron range are intended. Though this implies stronger geometry dependence, this latter effect is, in principle, under clean theoretical control, since it follows directly from quantum field theory [18].

Straightforward computations of geometry dependencies are conceptually complicated, since the relevant information is subtly encoded in the fluctuation spectrum. Analytic solutions can usually be found only for highly symmetric geometries. This problem is particularly prominent, since current and future precision measurements predominantly rely on configurations involving curved surfaces, such as a sphere above a plate. As a general recipe, the proximity-force approximation (PFA) [19] has been the standard tool for estimating curvature effects for nonplanar geometries in all experiments so far. The fact that the PFA is uncontrolled with unknown validity limits makes this approach highly problematic.

Therefore, a technique is needed that facilitates Casimir computations from field-theoretic first principles. For this purpose, *world-line numerics* has been developed [20], combining the string-inspired approach to quantum field theory [21] with Monte Carlo methods. As a main advantage, the world-line algorithm can be formulated for arbitrary geometries, resulting in a numerical estimate of the exact answer [22]. For the sphere-plate and cylinder-plate configurations, also new analytic methods are currently developed and latest results including exact solutions are given in [23,24]. In either case, quantitatively accurate results for the experimentally relevant parameter ranges are missing so far.

In this Letter, we use world-line numerics [20,22] to examine the Casimir effect in a sphere-plate and cylinder-plate geometry for a fluctuating scalar field, obeying Dirichlet boundary conditions (''Dirichlet scalar''). We compute the Casimir interaction energies that give rise to forces between the rigid surfaces. Thereby, we quantitatively determine validity bounds for the PFA. Apart from numerical discretization, for which a careful error management on the 0.1% level is performed, no quantum-field-theoretic approximation is needed.

We emphasize that the Casimir energies for the Dirichlet scalar should not be taken as an estimate for those for the electromagnetic (EM) field, leaving especially the sphere-plate case as a pressing open problem. Nevertheless, the validity constraints that we derive for the PFA hold independently of that, since the PFA approach makes no reference to the nature of the fluctuating field. If an experiment is performed outside the PFA validity ranges determined below, any comparison of the data with theory using the PFA has no firm basis.

Casimir curvature effects.—An intriguing property of the Casimir effect has always been its geometry dependence. As long as the typical curvature radii R_i of the surfaces are large compared to the surface separation a, the PFA is assumed to provide for a good approximation. In this approach, the curved surfaces are viewed as a superposition of infinitesimal parallel plates [17,19]. The Casimir interaction energy is obtained by an integration of the parallel-plate energy applied to the infinitesimal elements. Part of the curvature effect is introduced by the choice of a suitable integration measure which is generally ambiguous, as discussed, e.g., in [25]. For the case of a sphere with radius R at a (minimal) distance a from a plate, the PFA result at next-to-leading order reads

$$E_{\mathrm{PFA}}(a,R) = E^{(0)}_{\mathrm{PFA}}(a,R)\left(1 - \left\{\begin{matrix}1\\3\end{matrix}\right\} \times \frac{a}{R} + \mathcal{O}\left(\left(\frac{a}{R}\right)^2\right)\right), \tag{1}$$

$$E^{(0)}_{\mathrm{PFA}}(a,R) = -c_{\mathrm{PP}}\,\frac{\pi^3}{1440}\,\frac{R}{a^2}, \tag{2}$$

where the upper (lower) coefficient in braces holds for the so-called plate-based (sphere-based) PFA. They represent two limiting cases of the PFA and have often been assumed to span the error bars for the true result. Furthermore, $c_{\mathrm{PP}} = 2$ for an EM field or a complex scalar, and $c_{\mathrm{PP}} = 1$ for real scalar-field fluctuation.

Heuristically, the PFA is in contradiction with Heisenberg's uncertainty principle, since the quantum fluctuations are assumed to probe the surfaces only locally at each infinitesimal element. However, fluctuations are not localizable, but at least probe the surface in a whole neighborhood. In this manner, the curvature information enters the fluctuation spectrum. This quantum mechanism is immediately visible in the world-line formulation of the Casimir problem. Therein, the sum over fluctuations is mapped onto a Feynman path integral. Each path (world line) can be viewed as a random spacetime trajectory of a quantum fluctuation. Owing to a generic spatial extent of the world lines, the path integral directly samples the curvature properties of the surfaces [22].

For the Dirichlet scalar, the world-line representation of the Casimir interaction energy boils down to [22,26]

$$E_{\mathrm{Casimir}} = -\frac{1}{2}\,\frac{1}{(4\pi)^2}\int_0^\infty \frac{dT}{T^3}\,e^{-m^2T}\langle\Theta_\Sigma[x]\rangle_x. \tag{3}$$

Here, energy densities of the single bodies which are separation independent and thus do not contribute to the force are already subtracted [27]. The expectation value in (3) has to be taken with respect to an ensemble of closed world lines,

$$\langle\cdots\rangle_x := \int_{x(T)=x(0)} \mathcal{D}x\cdots e^{-(1/4)\int_0^T d\tau\dot{x}^2}, \tag{4}$$

with implicit normalization $\langle 1\rangle_x = 1$. In Eq. (3), $\Theta_\Sigma[x] = 1$ if a world line x intersects both surfaces $\Sigma = \Sigma_1 + \Sigma_2$, and $\Theta_\Sigma[x] = 0$ otherwise. A world line with $\Theta_\Sigma[x] = 1$ represents a boundary-condition violating fluctuation. Its removal from the set of admissible fluctuations contributes to the negative Casimir interaction energy.

We evaluate the world-line integral with Monte Carlo techniques, generating an ensemble of n_{L} world lines with the *worldline numerics* algorithm [22]. Each world line is characterized by N points after discretizing its proper time. In this work, we have used ensembles with up to $n_{\mathrm{L}} = 2.5\times10^5$ and $N = 4\times10^6$. Details of the algorithmic improvements used for this work will be given elsewhere [28].

Further advanced field-theoretic methods have been developed for Casimir calculations during the past years. Significant improvements compared to the PFA have been achieved by the semiclassical approximation [29], a functional-integral approach using boundary auxiliary fields [30], and the optical approximation [25]. These methods are especially useful for analyzing particular geometries by purely or partly analytical means; in the general case, approximations are often necessary but difficult to control. Hence, our results can also shed light on the quality of such approximations.

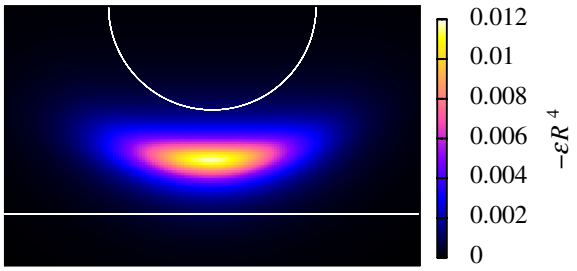

FIG. 1 (color online). Contour plot of the negative Casimir interaction energy density for a sphere of radius R above an infinite plate; the sphere-plate separation a has been chosen as $a = R$ here. The plot results from a pointwise evaluation of Eq. (3) using world lines with a common center of mass.

Sphere above plate.—We consider a sphere with radius R above an infinite plate at a (minimal) distance a. A contour plot of the energy density along a radial plane obtained by a pointwise evaluation of Eq. (3) is shown in Fig. 1. This density is related to the density of world lines with a given center of mass that intersects both surfaces. Figure 2 presents a global view on the Casimir interaction energy for a wide range of the curvature parameter a/R; the energy is normalized to the zeroth order of the PFA formula (2), $E^{(0)}_{\mathrm{PFA}}$. For small a/R ("large spheres"), our world-line result (crosses with error bars) and the full sphere- and plate-based PFA estimates (dashed-dotted lines) show reasonable agreement, settling at the zeroth-order PFA $E^{(0)}_{\mathrm{PFA}}$. The first field-theoretic confirmation of

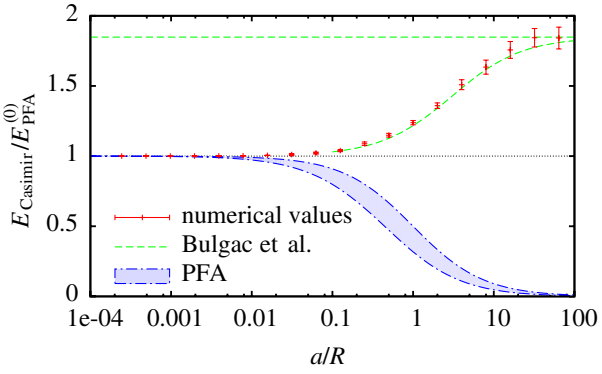

FIG. 2 (color online). Casimir interaction energy of a sphere with radius R and an infinite plate vs the curvature parameter a/R. The energy is normalized to the zeroth-order PFA formula (2), $E^{(0)}_{\mathrm{PFA}}$. For larger curvature parameter, the PFA estimate (dot-dashed line) differs qualitatively from the world-line result (crosses with error bars). Here, we observe good agreement of our result with the exact solution of [23] which is available for $a/R \gtrsim 0.1$ (dashed line).

this result has been obtained within the semiclassical approximation in [29]. The full PFA departs on the percent level from $E^{(0)}_{\rm PFA}$ for $a/R \gtrsim 0.01$, exhibiting a relative energy decrease. By contrast, our world-line result first stays close to $E^{(0)}_{\rm PFA}$ and then increases towards larger energy values relative to $E^{(0)}_{\rm PFA}$. This observation confirms earlier world-line studies [22] and agrees with the optical approximation [25] in this curvature regime.

For larger curvature $a/R \gtrsim 0.1$ (''smaller spheres''), we observe a strong increase relative to $E^{(0)}_{\rm PFA}$ [26]. Here, our data satisfactorily agree with the exact solution found recently for this regime [23] (dashed line). The latter work also provides for an exact asymptotic limit for $a/R \to \infty$, resulting in $180/\pi^4$ for our normalization. Our world-line data confirm this limit in Fig. 2.

Two important lessons can be learned from this plot: first, the PFA already fails to predict the correct sign of the curvature effects beyond zeroth order; see also [31]. Second, the relation between the Casimir effect for Dirichlet scalars and that for the EM field is strongly geometry dependent. For the parallel-plate case, Casimir forces only differ by the number of degrees of freedom; cf. the coefficient $c_{\rm PP}$ in Eq. (1). For large curvature, the Casimir energy for the Dirichlet scalar scales with a^{-2}, whereas that for the EM field obeys the Casimir-Polder law $\sim a^{-4}$ [32,33]. We emphasize that this difference does not affect our conclusions about the validity limits of the PFA, because the PFA makes no reference to the fluctuating field other than the coefficient $c_{\rm PP}$.

For a quantitative determination of the PFA validity limits, Fig. 3 displays the zeroth-order normalized energy for small-curvature parameter a/R. Here, our result has an accuracy of 0.1% (jackknife analysis). The error is dominated by the Monte Carlo sampling and the ordinary-integration accuracy; the error from the world-line discretization is found negligible in this regime, implying a sufficient proximity to the continuum limit.

In addition to our numerical error band, we consider the region between the sphere- and the plate-based PFA as the PFA error band. We identify the 0.1% accuracy limit of the PFA with the curvature parameter $a/R|_{0.1\%}$ where the two bands do no longer overlap. We obtain

$$\left.\frac{a}{R}\right|^{\rm PFA}_{0.1\%} \leq 0.00073 \qquad (5)$$

as the corresponding validity range for the curvature parameter. For instance, for a typical sphere with $R = 200\ \mu$m and an experimental accuracy goal of 0.1%, the PFA should not be used for $a \gtrsim 150$ nm. We conclude that the PFA should be dropped from the analysis of future experiments.

For the 1% accuracy limit of the PFA, we increase the band of our world-line estimate by this size and again determine the curvature parameter for which there is no intersection with the PFA band anymore. We obtain

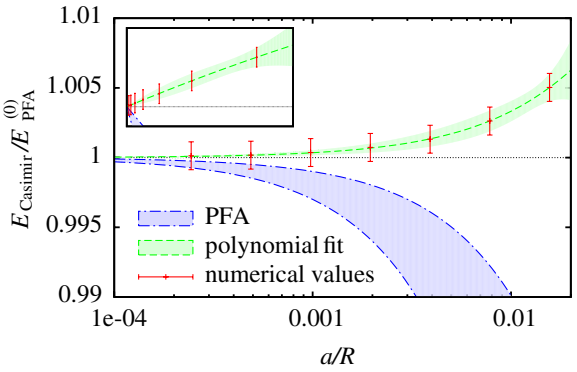

FIG. 3 (color online). Magnified view of Fig. 2 for small a/R. The 0.1% validity range of the PFA is characterized by curvature parameters, where the error band of our world-line results and the PFA band (blue-shaded or in between the dot-dashed lines) overlap; see Eq. (5). The dashed lines depict a constraint polynomial fit of the world-line result, $p(a/R) = 1 + 0.35(a/R) - 1.92(a/R)^2$, and its standard deviation. The inlay displays the same curves with a linear a/R axis.

$$\left.\frac{a}{R}\right|^{\rm PFA}_{1\%} \leq 0.00755. \qquad (6)$$

For a sphere with $R = 200\ \mu$m and an experimental accuracy goal of 1%, the PFA holds for $a < 1.5\ \mu$m. This result confirms the use of the PFA for the data analysis of the corresponding experiments performed so far.

In order to study the asymptotic expansion of the normalized energy, we fit our data to a second-order polynomial for $a/R < 0.1$ and include the exactly known result for $a/R \to 0$. We obtain $p(x) \simeq 1 + 0.35x - 1.92x^2 \pm 0.19x\sqrt{1 - 137.2x + 5125x^2}$, where $x = a/R$. The fit result is plotted in Fig. 3 (dashed lines), which illustrates that $E \simeq E^{(0)}_{\rm PFA} p(a/R)$ is a satisfactory approximation to the Casimir energy for $a/R < 0.1$, replacing the PFA (1). The inlay in this figure displays the same curves with a linear a/R axis, illustrating that the lowest-order curvature effect is linear in a/R. Given the results of the PFA (1), the semiclassical approximation [29], $p_{\rm sc}(x) \simeq 1 - 0.17x$, cf. [23], and the optical approximation [25], $p_{\rm opt}(x) \simeq 1 + 0.05x$, the latter appears to estimate curvature effects more appropriately.

Cylinder above plate.—The cylinder-plate configuration is a promising tool for high-precision experiments [34], since the force signal increases linearly with the cylinder length. Figure 4 shows the corresponding Casimir interaction energy versus the curvature parameter. The energy axis is again normalized to the zeroth-order PFA result, $E^{(0)}_{\rm PFA}(a, R) = -c_{\rm PP}\frac{\pi^3}{1920\sqrt{2}}\frac{R^{1/2}}{a^{5/2}}$. The qualitative conclusions for the validity of the PFA are similar to that for the sphere above a plate: beyond leading order, the PFA even predicts the wrong sign of the curvature effects. Quantitatively, the PFA validity limits are a factor ~ 3 larger than Eqs. (5) and (6), owing to the absence of curvature along the cylinder axis.

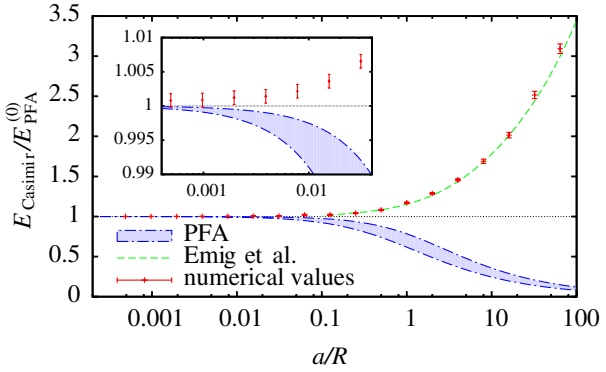

FIG. 4 (color online). Casimir interaction energy (normalized to $E^{(0)}_{\mathrm{PFA}}$) of an infinitely long cylinder with radius R at a distance a above an infinite plate vs the curvature parameter a/R. The inlay shows a magnified view for small values of a/R.

The most important difference to the sphere-plate case arises for large a/R. Here, the data are compatible with a loglike increase relative to $E^{(0)}_{\mathrm{PFA}}$, implying a surprisingly weak decrease of the Casimir force for large curvature $a/R \to \infty$. Our result agrees nicely with the very recent exact result [24] which is available for $a/R \gtrsim 0.1$. The data thus confirm the observation of [24] that the resulting Casimir force has the weakest possible decay, $F \sim 1/[a^3 \ln(a/R)]$, for asymptotically large curvature parameter $a/R \to \infty$.

In summary, we have computed Casimir interaction energies for the sphere-plate and cylinder-plate configuration with Dirichlet boundary conditions from first principles for a wide range of curvature parameters a/R. In general, we observe that curvature effects and geometry dependencies are intriguingly rich, implying that naïve estimates can easily be misguiding. In particular, predictions based on the PFA are only reliable in the asymptotic no-curvature limit. Its quantitative validity bounds given above and thus genuine Casimir curvature effects are in reach of currently planned experiments. Then, of course, finite-conductivity, surface-roughness, and thermal corrections also have to be accounted for on this level of precision [14–17]. For the ''low-curvature'' experiments performed so far, our results confirm that the use of the PFA for the data analysis was appropriate.

Beyond the Dirichlet scalar investigated here, it is well possible, e.g., for the EM field, that some cancellation of curvature effects occurs between modes obeying different boundary conditions. In fact, such a partial cancellation between TE and TM modes of the separable cylinder-plate geometry can be observed in the recent exact result for the EM field for small curvature [24]. Casimir calculations for the EM field in nonseparable geometries, such as the important sphere-plate case, therefore remain a prominent open problem.

The authors are grateful to T. Emig, R. L. Jaffe, A. Scardicchio, and A. Wirzba for useful discussions. The authors acknowledge support by the DFG under Contracts No. Gi 328/1-3 (Emmy-Noether program) and No. Gi 328/3-2.

Note added.—In the cylinder-plate case, an analytic small-curvature solution was found quite recently by Bordag [35]; his result and ours are perfectly compatible.

[1] H. B. G. Casimir, Kon. Ned. Akad. Wetensch. Proc. **51**, 793 (1948).
[2] S. K. Lamoreaux, Phys. Rev. Lett. **78**, 5 (1997).
[3] U. Mohideen and A. Roy, Phys. Rev. Lett. **81**, 4549 (1998).
[4] A. Roy *et al.*, Phys. Rev. D **60**, 111101(R) (1999).
[5] T. Ederth, Phys. Rev. A **62**, 062104 (2000).
[6] H. B. Chan *et al.*, Science **291**, 1941 (2001).
[7] G. Bressi *et al.*, Phys. Rev. Lett. **88**, 041804 (2002).
[8] F. Chen *et al.*, Phys. Rev. Lett. **88**, 101801 (2002).
[9] M. Bordag *et al.*, Phys. Rev. D **58**, 075003 (1998); **60**, 055004 (1999); **62**, 011701 (2000).
[10] J. C. Long *et al.*, Nucl. Phys. **B539**, 23 (1999).
[11] V. M. Mostepanenko and M. Novello, Phys. Rev. D **63**, 115003 (2001).
[12] K. A. Milton *et al.*, Mod. Phys. Lett. A **16**, 2281 (2001).
[13] R. S. Decca *et al.*, Phys. Rev. D **68**, 116003 (2003); R. S. Decca *et al.*, Phys. Rev. Lett. **94**, 240401 (2005).
[14] G. L. Klimchitskaya *et al.*, Phys. Rev. A **60**, 3487 (1999).
[15] A. Lambrecht and S. Reynaud, Eur. Phys. J. D **8**, 309 (2000).
[16] V. B. Bezerra *et al.*, Phys. Rev. A **62**, 014102 (2000).
[17] M. Bordag *et al.*, Phys. Rep. **353**, 1 (2001).
[18] N. Graham *et al.*, Nucl. Phys. **B645**, 49 (2002).
[19] B. V. Derjaguin *et al.*, Q. Rev. Chem. Soc. **10**, 295 (1956); J. Blocki, J. Randrup *et al.*, Ann. Phys. (N.Y.) **105**, 427 (1977).
[20] H. Gies and K. Langfeld, Nucl. Phys. **B613**, 353 (2001); Int. J. Mod. Phys. A **17**, 966 (2002).
[21] See, e.g., C. Schubert, Phys. Rep. **355**, 73 (2001).
[22] H. Gies *et al.*, J. High Energy Phys. 06 (2003) 018; hep-th/0311168.
[23] A. Bulgac *et al.*, Phys. Rev. D **73**, 025007 (2006); A. Wirzba *et al.*, J. Phys. A **39**, 6815 (2006).
[24] T. Emig *et al.*, **96**, 080403 (2006).
[25] R. L. Jaffe and A. Scardicchio, Nucl. Phys. **B704**, 552 (2005); Phys. Rev. Lett. **92**, 070402 (2004).
[26] H. Gies and K. Klingmüller, J. Phys. A **39**, 6415 (2006).
[27] K. A. Milton, *The Casimir Effect: Physical Manifestations of Zero-Point Energy*, (World Scientific, Singapore, 2001).
[28] H. Gies and K. Klingmüller, quant-ph/0605141.
[29] M. Schaden and L. Spruch, Phys. Rev. A **58**, 935 (1998); Phys. Rev. Lett. **84**, 459 (2000).
[30] R. Golestanian and M. Kardar, Phys. Rev. A **58**, 1713 (1998); T. Emig *et al.*, Phys. Rev. Lett. **87**, 260402 (2001); T. Emig and R. Buscher, Nucl. Phys. **B696**, 468 (2004).
[31] I. Brevik *et al.*, J. Phys. A **38**, L49 (2005).
[32] H. B. G. Casmir and D. Polder, Phys. Rev. **73**, 360 (1948).
[33] V. Druzhinina and M. DeKieviet, Phys. Rev. Lett. **91**, 193202 (2003).
[34] M. Brown-Hayes *et al.*, Phys. Rev. A **72**, 052102 (2005).
[35] M. Bordag, hep-th/0602295.